

# Design, synthesis and biological evaluation of novel 1,2,3-triazolyl $\beta$ -hydroxy alkyl/carbazole hybrid molecules

Mohammad Navid Soltani Rad<sup>1</sup> · Somayeh Behrouz<sup>1</sup> · Marzieh Behrouz<sup>1</sup> · Akram Sami<sup>1</sup> · Mehdi Mardkhoshnood<sup>2</sup> · Ali Zarenezhad<sup>2</sup> · Elham Zarenezhad<sup>2</sup>

Received: 3 November 2015 / Accepted: 22 May 2016  
© Springer International Publishing Switzerland 2016

**Abstract** The design, synthesis and biological study of several novel 1,2,3-triazolyl  $\beta$ -hydroxy alkyl/carbazole hybrid molecules as a new type of antifungal agent has been described. In this synthesis, the *N*-alkylation reaction of carbazol-9-ide potassium salt with 3-bromoprop-1-yne afforded 9-(prop-2-ynyl)-9*H*-carbazole. The ‘Click’ Huisgen cycloaddition reaction of 9-(prop-2-ynyl)-9*H*-carbazole with diverse  $\beta$ -azido alcohols in the presence of copper-doped silica cuprous sulphate led to target molecules in excellent yields. The *in vitro* antifungal and antibacterial activities of title compounds were screened against various pathogenic fungal strains, Gram-positive and/or Gram-negative bacteria. In particular, 1-(4-((9*H*-carbazol-9-yl) methyl)-1*H*-1,2,3-triazol-1-yl)-3-butoxypropan-2-ol (**10e**) proved to have potent antifungal activity against all fungal tests compared with fluconazole and clotrimazole as studied reference drugs. Our molecular docking analysis revealed an appropriate fitting and a potential powerful interaction between compound **10e** and an active site of the Mycobacterium P450DM enzyme. The strong hydrogen bondings between  $\beta$ -hydroxyl and ether groups in **10e** were found to be the main factors that drive the molecule to fit in the active site of enzyme. The *in silico* pharmacokinetic studies were used for

a better description of **10a–10n** as potential lead antifungal agents for future investigations.

**Keywords** Antifungal · Antibacterial · Carbazole ·  $\beta$ -Hydroxy 1, 2, 3-triazole · Mycobacterium P450DM

## Introduction

Infections caused by pathogenic microorganisms are still a continuous and serious threat to human life worldwide [1]. Typically, the infections caused by opportunistic fungal pathogens are a well-known reason for morbidity in patients with impaired immune system, such as patients undergoing organ transplants, HIV and cancer chemotherapy [2–5]. Up to now, numerous antifungal agents with different modes of action mechanism have been developed for medical uses [6]. However, the medical care with current antifungal drugs is limited for several reasons including resistance against fungal species, toxicity, pharmacokinetic deficiencies and undesirable side effects [7, 8]. In the last decades, the growing concerns about antifungal drugs have created a substantial need for developing newer types of antifungal drugs. In this connection, extensive efforts have been made to design and synthesize new antifungal agents with a wide spectrum of activities.

The azole derivatives are known for exhibiting good bioavailability, high therapeutic index, favourable safety profile and low toxicity [9, 10]. It is well established that azole cores in most azole antifungal drugs are the main pharmacophoric sites for establishing antifungal activity. Ergosterol is an essential component for constructing the cell membrane in fungi cells. It is well indicated that azole antifungals inhibit biosynthesis of ergosterol via the coordination with the iron core present in the haem cofactor at the active site

**Electronic supplementary material** The online version of this article (doi:10.1007/s11030-016-9678-7) contains supplementary material, which is available to authorized users.

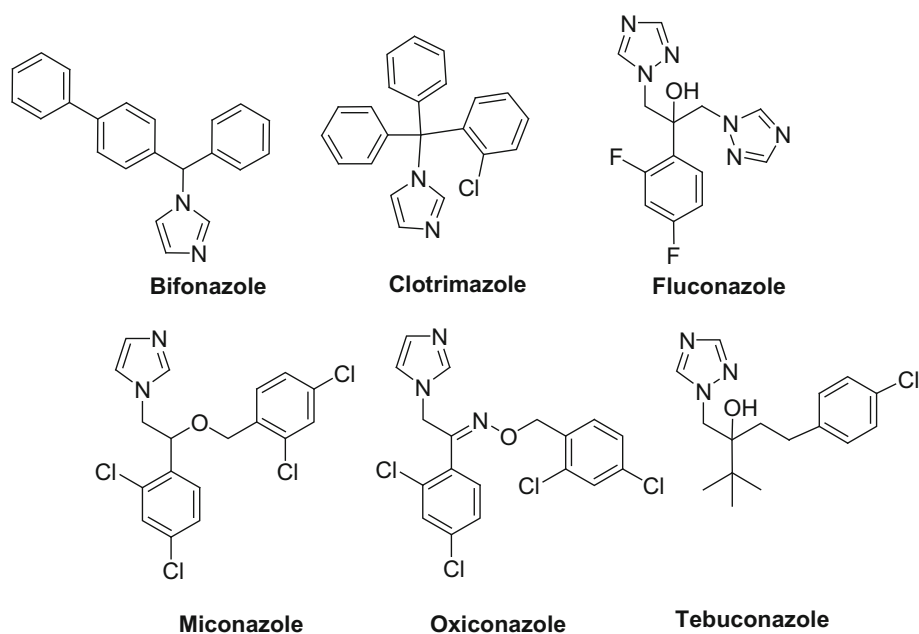
✉ Mohammad Navid Soltani Rad  
soltani@sutech.ac.ir

✉ Somayeh Behrouz  
behrouz@sutech.ac.ir

<sup>1</sup> Department of Chemistry, Shiraz University of Technology, 71555-313 Shiraz, Iran

<sup>2</sup> Fasa University of Medical Sciences, Fasa, Iran

**Fig. 1** Structures of several clinically used azole antifungals



of cytochrome P450-dependent 14  $\alpha$ -lanosterol demethylase (CYP51, P45014DM) [11]. This enzyme has an essential role in biosynthesis of ergosterol and hence can be considered as a favourable target for most azole antifungal drugs [11–13]. The structures of several clinically used azole antifungals are shown in Fig. 1.

From recent advances in Cu(I)-catalyzed azide-alkyne cycloaddition (CuAAC) for regioselective synthesis of 1,4-disubstituted 1,2,3-triazoles, 1,2,3-triazole rings have emerged as ideal surrogates or bioisosteres of previously identified azole cores of well-established antifungals [14,15]. 1,2,3-Triazole derivatives display a wide range of biological activities, such as antibiotic, antiviral, anti-allergic, anti-inflammatory, anticancer, and antifungal [6,16].

Affinity of 1,2,3-triazolyl cores to bind at the surface of receptors or enzymes is contributed by the potential to undergo hydrogen bonding, dipole-dipole, as well as hydrophobic interactions with the target biomolecules [17]. Thus, the incorporation of 1,2,3-triazolyl cores into the scaffolds of bioactive molecules is interesting [16,18].

In recent years, the drug design based on molecular hybridization has attracted massive interests in medicinal chemistry. Due to this approach, two bioactive pharmacophores are conjugated through a spacer into a single structure to behave as dual-acting drugs and/or to lessen the side effects [19,20]. Carbazole-triazole hybrid molecules have found extensive applications in the design and synthesis of many carbazole-triazole hybrid-based drugs, drug candidates [21–26] and optoelectronic devices [27–30]. To this end, the carbazole-triazole hybrid moieties have been widely applied in scaffolds of many molecules exhibiting

diverse pharmaceutical properties. The structures and properties of some carbazole-triazole hybrid molecules are shown in Figs. 2 and 3.

Formerly, the triazole-carbazole hybrid molecules **6–9** were reported as promising molecules having apparent antibacterial and antifungal activities (Fig. 3) [25,26,31,32]. Therefore, with inspiration from the remarkable biological activities of 1,2,3-triazole and carbazole and also in continuation of our interest in discovering the new azole bioactive compounds [33–40], herein we would like to report the design and synthesis of some 1,2,3-triazolyl  $\beta$ -hydroxy alkyl/carbazole hybrids as a new type of antifungal agent (Fig. 3). In this synthesis, 1,2,3-triazole cores were conjugated with carbazole through CuAAC to achieve the novel hybrid molecules **10a–10n**. As shown in Fig. 3, our new compounds (**10a–10n**) have structural resemblance to compounds **7–9** with a main difference that our compounds have the  $\beta$ -hydroxyl moiety. It is assumed that the presence of this hydroxyl group can increase the binding affinity of our compounds to active sites of enzyme or receptors [41].

## Results and discussion

### Chemistry

The synthetic route to access **10a–10n** is achieved by the general pathway illustrated in Schemes 1, 2, 3 and 4. As shown in Scheme 1, the first step includes the preparation of 9-(prop-2-ynyl)-9*H*-carbazole (**12**), which is a key starting material for Huisgen's azide-alkyne cycloaddition. The

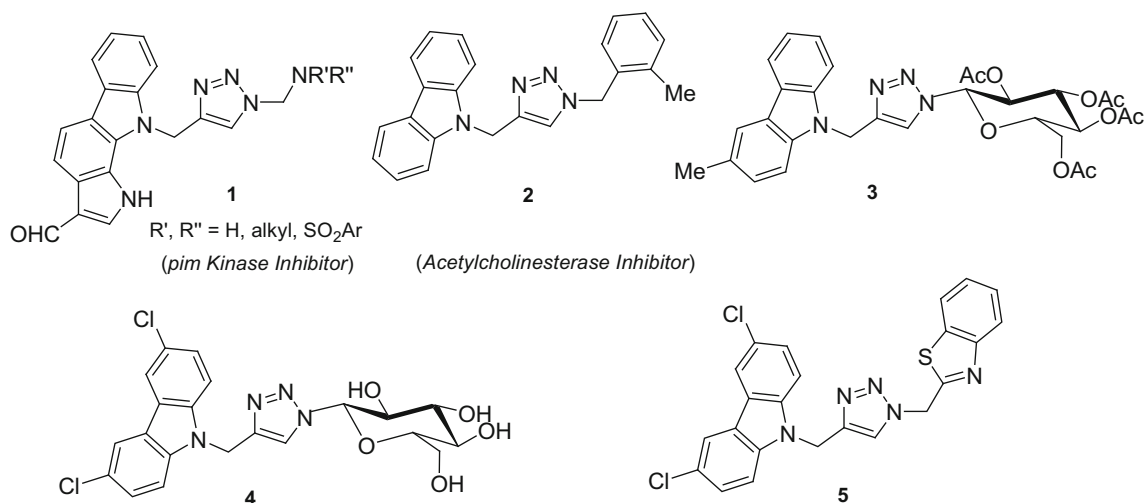
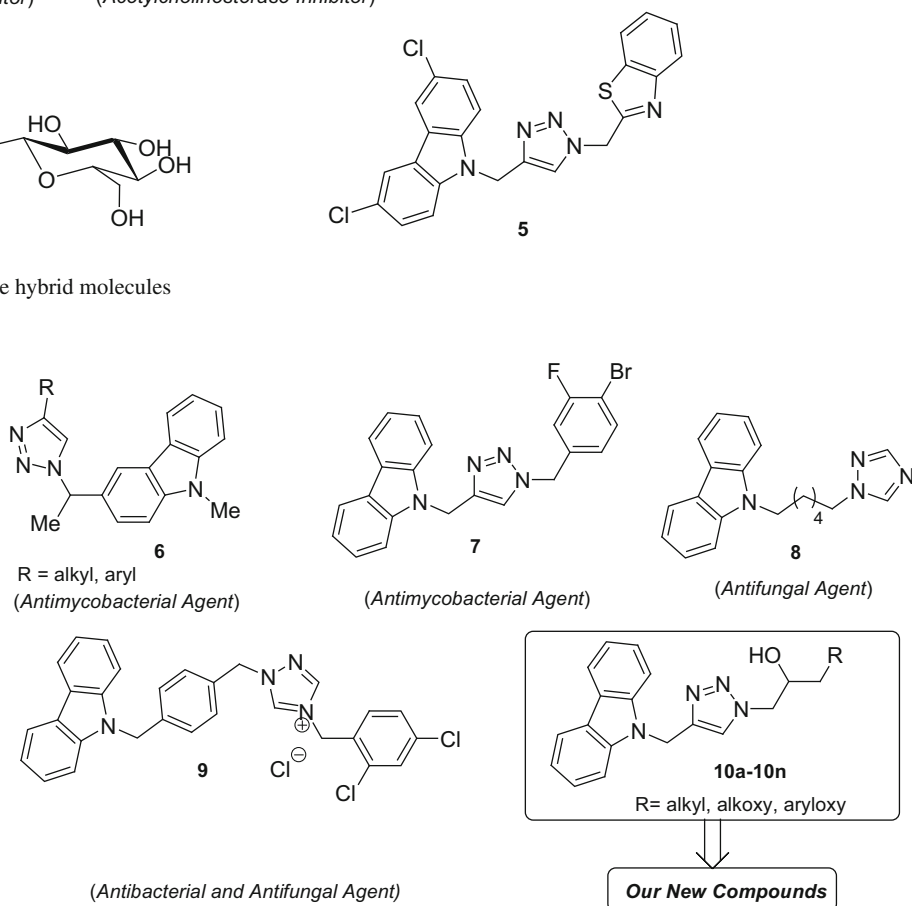
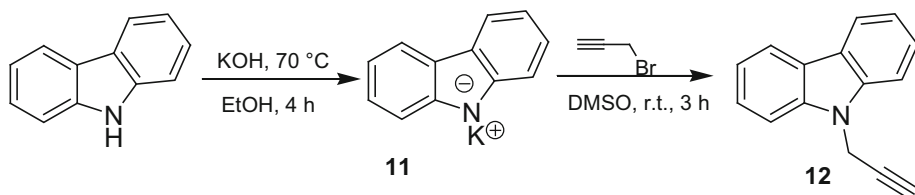


**Fig. 2** Structures of some carbazole-triazole hybrid molecules

**Fig. 3** Structures and biological properties of triazole-carbazole hybrids **6–9** and general structure of 1,2,3-triazolyl  $\beta$ -hydroxy alkyl/carbazole hybrid molecules **10a–10n**

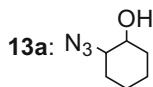
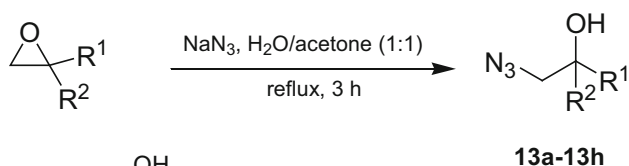


**Scheme 1** Synthesis of 9-(prop-2-ynyl)-9H-carbazole (**12**)



synthesis of alkyne **12** was previously reported by different groups [42,43]. However, utilization of the reported procedures resulted in unsatisfactory yields of **12**. Thus, we considered an alternative procedure in which alkyne **12** was simply prepared from reaction of 3-bromoprop-1-yne with carbazole potassium salt **11** in DMSO at ambient temperature for 3 h (94%). It is worth mentioning that carbazole salt **11** was earlier prepared by dissolving 9H-carbazole in a KOH/EtOH solution followed by heating at 70 °C for 4 h.

In the second step, the desired organic azides were synthesized (Scheme 2). In the design of **10a–10n**, the use of  $\beta$ -azido alcohols was preferred to simple alkyl azides, since the presence of a hydroxyl group may drive the molecule to the active site of enzyme via hydrogen bonds and dipole interactions. In this context, several structurally diverse  $\beta$ -azido alcohols **13a–13n** bearing various substituents were prepared by regioselective ring opening of the corresponding epoxides with  $\text{NaN}_3$  [44] (Schemes 2, 3).



**13b:** R<sup>1</sup>=Me, R<sup>2</sup>=H

**13c:** R<sup>1</sup>=Et, R<sup>2</sup>=H

**13d:** R<sup>1</sup>=Me, R<sup>2</sup>=Me

**13e:** R<sup>1</sup>=CH<sub>2</sub>OBu, R<sup>2</sup>=H

**13f:** R<sup>1</sup>=CH<sub>2</sub>OCHMe<sub>2</sub>, R<sup>2</sup>=H

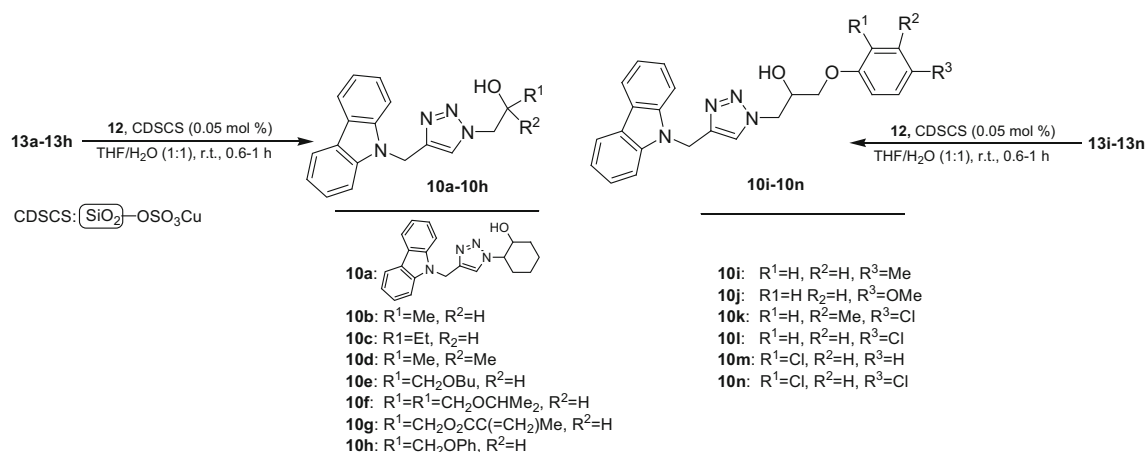
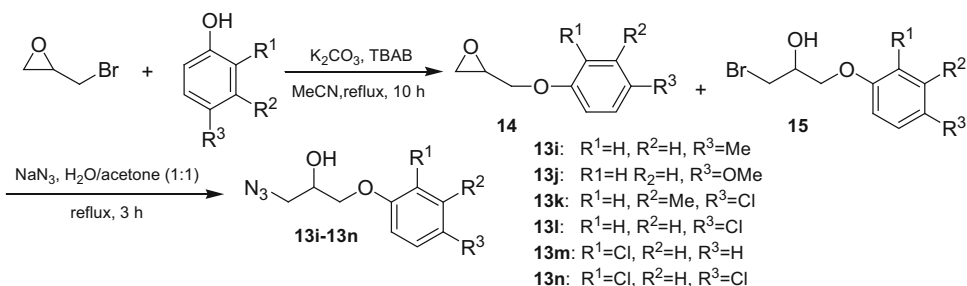
**13g:** R<sup>1</sup>=CH<sub>2</sub>O<sub>2</sub>CC(=CH<sub>2</sub>)Me, R<sup>2</sup>=H

**13h:** R<sup>1</sup>=CH<sub>2</sub>OPh, R<sup>2</sup>=H

**Scheme 2** Synthesis of  $\beta$ -azido alcohols **13a–13h**

Since some starting epoxides used in this synthesis were not commercially available, two different pathways were employed to produce **13a–13n**. Compounds **13a–13h** were prepared in racemic forms due to Scheme 2 by coupling of NaN<sub>3</sub> with the desired non-chiral epoxides in refluxing acetone/H<sub>2</sub>O (1:1). In this reaction condition, NaN<sub>3</sub> normally attacks the less hindered C-atom of the terminal epoxide.

**Scheme 3** Synthesis of  $\beta$ -azido alcohols **13i–13n**



**Scheme 4** CuAAC of 9-(prop-2-ynyl)-9H-carbazole (**12**) and  $\beta$ -azido alcohols (**13a–13n**)

residues. Different substituents comprising alkyl (**10a–10d**), alkoxy (**10e**, **10f**), methacrylate ester (**10g**) and aryloxy residues (**10h–10n**) were considered in the structure of title compounds.

### Antifungal and antibacterial studies

The in vitro antifungal activity for 1,2,3-triazolyl  $\beta$ -hydroxy alkyl/carbazole hybrid molecules **10a–10n** was assessed against some pathogenic fungi comprising *Candida albicans* (ATCC 10231), *Candida krusei* (ATCC 6258), *Aspergillus niger* (ATCC 16404) and *Trichophyton rubrum* (PTCC 5143). In addition, all compounds were also screened against two pathogenic bacteria including *Staphylococcus aureus* (PTCC 1133) and *Escherichia coli* (PTCC 1330). For both antifungal and antibacterial activities, the MIC<sub>50</sub> (minimum inhibitory concentration,  $\mu\text{g/mL}$ ) values were reported according to protocols established by the Clinical and Laboratory Standards Institute, USA (formerly the National Committee for Clinical Laboratory Standards) [45]. The tested fungal and bacteria strains were obtained either from the American Type Culture Collection (ATCC) or the Persian Type Culture Collection (PTCC). The MIC<sub>50</sub> values were determined for **10a–10n** using serial dilution method in DMSO as a solvent. The sterile growth mediums including Sabouraud dextrose broth and Muller–Hinton agar were used for fungal and bacteria tests, respectively.

The MIC<sub>50</sub> values were recorded in a culture with turbidity <50% inhibition relative to the growth of the control. The fungal and bacteria strains were incubated at 37 °C, and the growth MIC<sub>50</sub> was determined at different times (12, 24, 36 and 48 h). As can be seen in Table 1, **10e** was the most potent agent against all tested fungal pathogens and proved to have a broad activity for all studied fungal strains and its reactivity is comparable with clotrimazole and fluconazole as reference drugs. For *T. rubrum*, **10e** even was more potent than fluconazole. Except that of *C. Krusei*, **10d** also exhibited similar reactivity to **10e** against all tested fungal organisms. Although **10b** was inactive against *C. albicans*; however, it proved to have an efficient activity against all examined fungi. Compounds **10f**, **10g**, **10i**, **10k** and **10m** showed the selective antifungal activity against some tested fungal pathogens. The other tested compounds were inactive or displayed marginal activity. From the structure activity relationship standpoint, since **10a–10n** only varies in side chains; therefore, the differences in antifungal activities are attributed to these variations. In general, it is assumed that the presence of aliphatic side chains showed more satisfactory result in comparison with aryl moieties even bearing different substituents.

All compounds were also screened to indicate their antibacterial activities. In this connection, two pathogenic

**Table 1** In vitro antibacterial and antifungal study of **10a–10n**

Compd.	MIC <sub>50</sub> ( $\mu\text{g/mL}$ ) <sup>a</sup>					
	S.A.	E.C.	C.A.	C.K.	A.N.	T.R.
<b>10a</b>	6.25	12.5	12.5	12.5	100	25
<b>10b</b>	6.25	6.25	6.25	3.125	25	6.25
<b>10c</b>	1.562	3.125	6.25	12.5	50	50
<b>10d</b>	12.5	25	1.562	6.25	25	3.125
<b>10e</b>	12.5	12.5	1.562	3.125	25	6.25
<b>10f</b>	12.5	3.125	12.5	3.125	100	25
<b>10g</b>	6.25	12.5	6.25	12.5	100	12.5
<b>10h</b>	12.5	6.25	6.25	25	50	50
<b>10i</b>	1.562	12.5	6.25	12.5	12.5	6.25
<b>10j</b>	12.5	12.5	3.125	12.5	50	12.5
<b>10k</b>	6.25	1.562	12.5	6.25	50	12.5
<b>10l</b>	6.25	12.5	12.5	6.25	100	50
<b>10m</b>	3.125	25	3.125	6.25	25	12.5
<b>10n</b>	6.25	6.25	12.5	12.5	50	25
Ampi. <sup>b</sup>	0.781	–	–	–	–	–
Gent. <sup>c</sup>	–	0.781	–	–	–	–
Clot. <sup>d</sup>	–	–	1.562	3.125	25	6.25
Fluc. <sup>d</sup>	–	–	1.562	3.125	25	12.5

Examined bacteria: S.A. *Staphylococcus aureus* (PTCC 1133) and E.C. *Escherichia coli* (PTCC 1330); Tested fungi: C.A. *Candida albicans* (ATCC 10231), C.K. *Candida krusei* (ATCC 6258), A.N. *Aspergillus niger* (ATCC 16404), T.R. *Trichophyton rubrum* (PTCC 5143)

<sup>a</sup> Minimum inhibitory concentration

<sup>b</sup> Ref. drug for Gram-positive bacteria: Ampi. ampicillin

<sup>c</sup> Ref. drug for Gram-negative bacteria: Gent. gentamycin

<sup>d</sup> Reference drugs for fungal species: Clot. clotrimazole, Fluc. fluconazole

bacteria were studied namely *Staphylococcus aureus* (PTCC 1133) and *Escherichia coli* (PTCC 1330) as representatives for Gram-positive and Gram-negative bacteria, respectively.

Gentamycin and ampicillin were used as reference drugs for Gram-negative and Gram-positive bacteria, respectively. As the data in Table 1 indicate, most of the examined compounds have negligible antibacterial activity against both tested bacteria as compared to the standard drugs. In this context, only **10c** proved to have the promising antibacterial activity against both studied bacteria to some extent.

### Molecular docking study

Molecular docking study is an attractive method to predict the interactions of the new drug candidates with the target enzyme and/or receptor binding sites. Since **10e** was determined as the most potent antifungal agent, thus the binding mode of **10e** in the active site of cytochrome P450-dependent 14  $\alpha$ -lanosterol demethylase was investi-

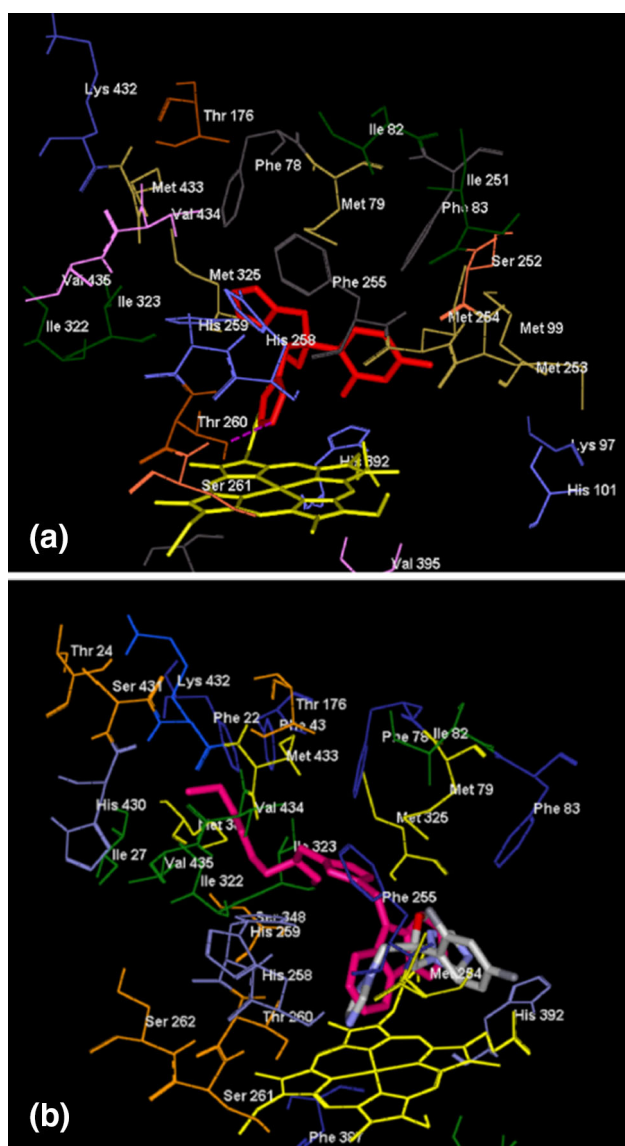


**Fig. 4** **a** Hydrogen bonding of fluconazole (*red*) in active site of Mycobacterium P450DM, **b** Combined view of docked conformation of fluconazole (*grey*) and compound **10e** (*pink*) in active site of Mycobacterium P450DM. (Color figure online)

gated carrying out a molecular docking study. For this, the crystal structure of the enzyme (from Mycobacterium tuberculosis; Mycobacterium P450DM) in complex with fluconazole (PDB code: 1EA1) was selected as the template which was retrieved from the Protein Data Bank (<http://www.rcsb.org>). Molegro Virtual Docker (MVD) software was employed using its default settings to carry out the docking study [46].

The enzyme was then modified by removing all water molecules and other present ligands. The active site of the enzyme was defined to comprise the residues within a 7 Å radius around the bound inhibitor. The DFT method at the B3LYP/6-311+G\*\* level of theory was used to assign

the optimized geometry of **10e**. Initially, fluconazole was redocked at the active site of enzyme to validate our docking protocol (Fig. 4). As reported previously, the root-mean-square deviation (RMSD) values should be  $<2 \text{ \AA}$  [47]. Using the MVD software, the RMSD value between the docked and co-crystallized fluconazole was found to be 1.34 Å which confirms our docking protocol.

Azole antifungals are capable to inhibit CYP51 through the binding to N-atoms in azoles with the iron core inside the haem. Podust and coworkers reported that the substrate-binding pocket of Mycobacterium P450DM is positioned above the porphyrin (haem) core [48]. This open pocket above the haem iron residue has a ceiling that consists of several lipophilic amino acid residues (Phe78, Met79, Phe83 and Phe255). In addition, access to pyrrole rings is restricted by Ala256, Thr260 and Leu321 [48]. In the case of fluconazole, the N4 of the 1,2,4-triazole moiety participates in a strong hydrogen bonding with Thr260. In addition, 1,2,4-triazole ring is positioned perpendicularly to the plane of porphyrin with distance of 3.56 Å between the N4 atom in the azole ring and the iron core of haem. Moreover, Phe83 and Phe255 also contribute in non-bonded interactions. Interestingly, similar to fluconazole, **10e** is accommodated at the same binding site and showed a strong interaction with the enzyme active site. Because of the similar functionalities in both **10e** and fluconazole, we expected a similar binding mode for **10e** with the enzyme as seen with fluconazole. Similar to other azole antifungal drugs, it was believed that binding of **10e** with the haem iron atom should be achieved through one of the N-atoms in the 1,2,3-triazole core; however, such an interaction was not observed. The 1,2,3-triazole ring usually demonstrates a weak binding affinity compared to the imidazole or 1,2,4-triazole moieties against the haem residue [49]. However, contrary to our expectations, the docking results revealed a higher binding affinity and thus a stronger interaction of **10e** with the enzyme compared with fluconazole. The calculated  $\Delta G$  values for fluconazole and **10e** are  $-88.42$  and  $-109.76$  (kcal/mol), respectively, indicating there is an energy gap of about 21.34 (kcal/mol). This energy gap attributes the stronger binding of **10e** at the active site of the enzyme. The binding geometry and interaction of **10e** with the active site of Mycobacterium P450DM are shown in Fig. 5.

Figure 5b clearly shows the hydrogen bondings of  $\beta$ -hydroxyl and ether moieties with Ile323 and Ile322. These hydrogen bond interactions play a critical role in the higher affinity of **10e** to the active site of the enzyme. The aliphatic side chain tethered to the triazole ring bound in a hydrophobic pocket above the haem group with residues including Ile27, Met79, Phe78, Ile82, Ile322, Ile323, Val434 and Val438. In addition, the bulky carbazole ring stands over the haem moiety in a way that its plane is perpendicular over the porphyrin

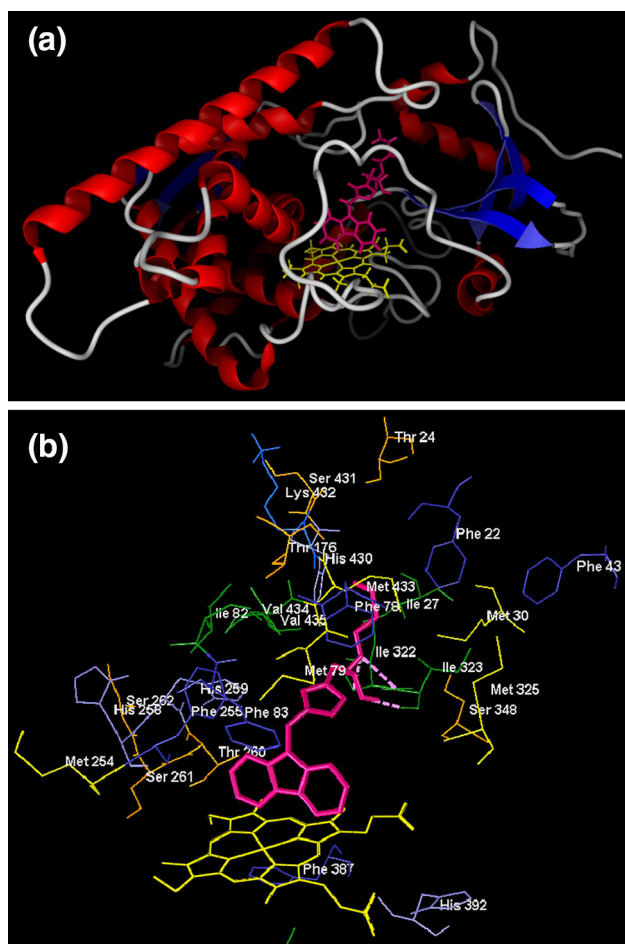


**Fig. 5** **a** Docked conformation of compound **10e** (pink) in active site of Mycobacterium P450DM, **b** Hydrogen bond of compound **10e** (pink) in the active site of Mycobacterium P450DM. (Color figure online)

plane. This spatial arrangement occupies the room over substrate access channel because of the presence of the carbazole ring. Thus, **10e** inhibits the Mycobacterium P450DM enzyme through a way which deviates from fluconazole known today as the ‘Umbrella’ effect [50]. In Fig. 6, the interaction of each fragment in **10e** specified by docking analysis is shown.

**Fig. 6** Role of each molecular fragment in **10e** for the inhibition of Mycobacterium P450DM as indicated by molecular docking

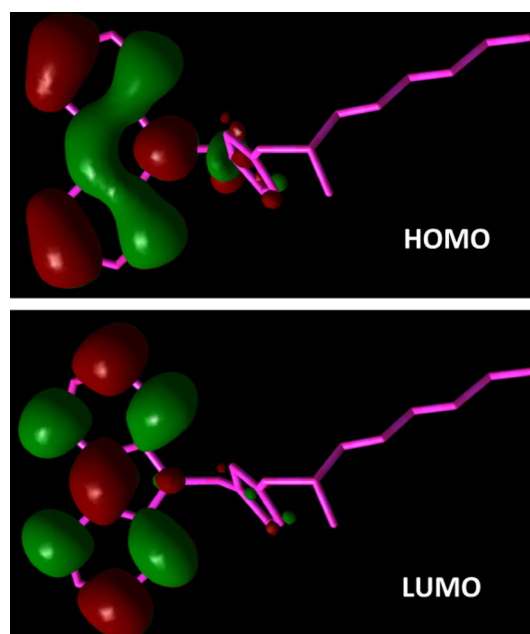
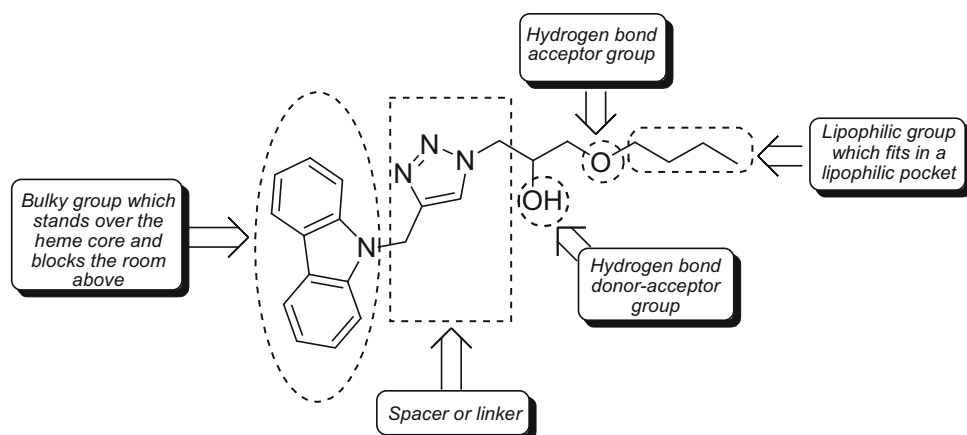


**Fig. 7** HOMO/LUMO view for the optimized geometry of **10e**

### Quantum study

To rationalize the higher binding affinity of **10e** compared to fluconazole in the active site of the enzyme, the energy of the highest occupied molecular orbital (HOMO) and the lowest unoccupied molecular orbital (LUMO) were calculated at the B3LYP/6–31G\*\* level of theory for the optimized structure of **10e** (Fig. 7).

In addition to the HOMO–LUMO energy level, we also calculated and compared the hardness and softness values for **10e** and fluconazole. The HOMO–LUMO energy gaps of 4.64 eV (HOMO =  $-5.72$  eV and LUMO =  $-1.08$  eV) and 6.16 eV (HOMO =  $-7.12$  eV and LUMO =  $-0.96$  eV) were obtained for **10e** and fluconazole, respectively (Table 2). This difference in HOMO–LUMO energy gap between **10e** and fluconazole indicates that **10e** is a softer molecule compared

**Table 2** Calculated HOMO, LUMO, hardness and softness of **10e** and fluconazole using B3LYP/6–31G\*\* level of theory

Ligand	HOMO <sup>a</sup>	LUMO <sup>a</sup>	Hardness <sup>a</sup>	Softness <sup>b</sup>
<b>10e</b>	−5.72	−1.08	2.32	0.43
Fluc.	−7.12	−0.97	3.08	0.32

<sup>a</sup> Unit in electron volt (ev)<sup>b</sup> Unit in ev<sup>−1</sup>

with fluconazole. Moreover, the calculated softness for **10e** also confirms a softer nature of **10e** in comparison with fluconazole. The softness of **10e** enhances its polarizability and thus may exhibit higher antagonistic activity compared with fluconazole.

#### *In silico pharmacokinetic profile, drug-likeness and toxicity predictions*

Nowadays many approaches based on in silico predictions like physicochemical properties, drug-likeness and toxicity risks for drug candidates have found extensive utility [51]. Since the initial findings by Lipinski, known today as Lipinski's rule of five (RO5) [52,53], various molecular descriptors and physicochemical parameters have been developed to predict the drug-likeness and toxicity risks of drug-like molecules. According to RO5, the key factors used to assess likelihood of oral absorption are (i) molecular weight (MW) <500 Dalton; (ii) A desired log *P* value (octanol-water partition coefficient) no more than 5; (iii) Not more than 5 hydrogen bond donors (sum of NH and OH); (iv) Not more than 10 hydrogen bond acceptors (sum of N and O) and (v) 10 or fewer rotatable bonds. Molecules that violate any of these rules may show sub-optimal pharmacokinetic properties for oral administration [52,53].

In this study, to assess the in silico pharmacokinetic profiles for **10a–10n**, we used validated open-source programs such as OSIRIS Property Explorer [54,55], Advanced Chemistry Development (ACD) [56], Marvin ChemAxon [57] and molinspiration property calculator [58], and then compared the results with those obtained for fluconazole and clotrimazole as reference drugs. The OSIRIS is an online program that works on the basis of molecular fragments. This software involves the database of traded drugs and commercially available compounds (none drug-like compounds). This program estimates the risks of side effects, such as mutagenic, tumorigenic, irritant and reproductive effects. The analysis of theoretical toxicity risks for **10a–10n** using OSIRIS program is summarized in Table 3. As can be seen in Table 3, **10a**, **10c**, **10d**, **10f**, **10h** and **10j** demonstrated the low risk of toxicity regarding to all studied parameters. Among these non-toxic agents, only **10d** and **10f** proved to have antifungal activity, whereas the other agents displayed weak activity against all

**Table 3** Toxicity risks predicted by OSIRIS Property Explorer for **10a–10n**

Compd.	Mutagenic	Tumorigenic	Irritant	Reproductive effect
<b>10a</b>	LR <sup>a</sup>	LR	LR	LR
<b>10b</b>	MR <sup>b</sup>	HR <sup>c</sup>	LR	LR
<b>10c</b>	LR	LR	LR	LR
<b>10d</b>	LR	LR	LR	LR
<b>10e</b>	LR	LR	HR	HR
<b>10f</b>	LR	LR	LR	LR
<b>10g</b>	HR	LR	HR	HR
<b>10h</b>	LR	LR	LR	LR
<b>10i</b>	LR	HR	LR	LR
<b>10j</b>	LR	LR	LR	LR
<b>10k</b>	LR	LR	LR	HR
<b>10l</b>	LR	LR	LR	HR
<b>10m</b>	LR	LR	MR	LR
<b>10n</b>	HR	HR	HR	HR
Fluc.	LR	LR	LR	MR
Clot.	LR	LR	LR	LR

<sup>a</sup> Low risk<sup>b</sup> Medium risk<sup>c</sup> High risk

tested fungal. The low risk for mutagenic and tumorigenic was determined for **10e** as the most potent antifungal agent, whereas it exhibited the high risk of toxicity due to its irritant and reproductive effect. The other studied compounds displayed low to high risk of toxicity (Table 3).

Using aforementioned programs, we also assessed the Lipinski's parameters as well as other descriptors for **10a–10n** (Table 4). As can be seen in Table 4, the number of hydrogen bond acceptors (nHba) = 3–5, number of hydrogen bond donors (nHbd) = 1 and number of rotatable bonds (nrotb) = 3–9 were almost similar to commercial drugs which lie in range of RO5. All computed molecular weights for **10a–10n** were also in range of 306–466 (<500 g/mol). The total polar surface area (TPSA) of a molecule is defined as the surface sum over all polar atoms, primarily oxygen and nitrogen and also including the attached hydrogen atoms. TPSA, as a molecular descriptor, is used to predict drug absorption, including intestinal absorption, bioavailability and blood–brain barrier penetration.

In most known drugs, TPSA values were calculated to be <140 Å<sup>2</sup>; in this regard, it was found that **10a–10n** exhibited the TSPA values between 55.87 to 82.17 Å<sup>2</sup>. Descriptors comprising clog *P*, log *S* and log *D* are critically important physicochemical parameters that indicate the drug's pharmacokinetic and the extent of drug delivery. An octanol–water partition coefficient clog *P* indicates the lipophilicity of a drug. Drugs with high lipophilicity value are unable to pass the blood–brain barrier. Most established drugs are known

**Table 4** Physicochemical properties predicted by OSIRIS Property Explorer, Advanced Chemistry Development (ACD), Marvin ChemAxon and Molinspiration Property Calculator for **10a–10n**

Compd.	nHba	nHbd	nrotb	TPSA	clog P	Log S	Log D	MW	MR	Drug-likeness	Drug score
<b>10a</b>	3	1	3	55.87	3.26	−3.29	3.57	346	103.46	−8.87	0.40
<b>10b</b>	3	1	4	55.87	1.96	−2.75	2.73	306	91.80	−5.51	0.21
<b>10c</b>	3	1	5	55.87	2.41	−3.02	3.19	320	96.32	−5.31	0.43
<b>10d</b>	3	1	4	55.87	2.34	−2.86	2.80	320	96.43	−5.66	0.44
<b>10e</b>	4	1	9	65.10	2.77	−3.21	3.43	378	111.96	−11.39	0.14
<b>10f</b>	4	1	7	65.10	2.22	−3.05	2.97	364	107.26	−3.43	0.43
<b>10g</b>	4	1	8	82.17	2.39	−2.99	3.80	390	111.50	−26.9	0.09
<b>10h</b>	4	1	7	65.10	2.98	−3.7	4.00	398	117.60	−2.69	0.40
<b>10i</b>	4	1	7	65.10	3.32	−4.05	4.47	412	122.64	−3.92	0.21
<b>10j</b>	5	1	8	74.33	2.91	−3.72	3.75	428	124.07	−2.56	0.38
<b>10k</b>	4	1	7	65.01	3.93	−4.78	4.98	446	127.45	−4.52	0.17
<b>10l</b>	4	1	7	65.01	3.58	−4.44	4.52	432	122.41	−1.32	0.23
<b>10m</b>	4	1	7	65.01	3.58	−4.44	4.52	432	122.41	−1.45	0.30
<b>10n</b>	4	1	7	65.01	4.19	−5.17	5.04	466	127.21	−1.42	0.04
Fluc.	5	1	5	81.65	−0.11	−2.17	−0.04	306	76.62	−1.13	0.46
Clot.	1	0	4	17.82	5.32	−7.72	5.60	344	102.14	0.92	0.30

to have clog *P* values <5. The calculated clog *P* values for **10a–10n** were around 1.96 to 4.19 which are below the threshold defined by RO5 (<5). Log *S* represents the aqueous solubility of a drug candidate that significantly affects its absorption and distribution characteristics. It is estimated that most recent drugs have a log *S* value > −4. As can be seen in Table 4, **10a–10h** and **10j** have log *S* values > −4. Log *D*, or distribution coefficient, is similar to log *P*; however, it is a pH-dependent parameter which normally is measured at the physiological pH. Bhal and coworkers have reported that log *D* can be a better descriptor for determining the lipophilicity factor in the context of the RO5 [59]. For non-ionisable compounds, log *D* and log *P*, at physiological pH are nearly the same. For **10a–10n**, the log *D* values vary from 2.73 to 5.04 and are within the acceptable RO5 range. Molar refractivity (MR) is a measure of the total polarizability of a drug depending on temperature, the index of refraction and the pressure. Most drug-like molecules have a molar refractivity between 40 and 130. A larger value of molar refractivity represents a larger molecular weight or volume in which enhances the polarizability as well as molecular softness values. When the molar refractivity increases, the drug-like molecule tends to have an antagonistic property. For **10a–10n**, their molar refractivity values were computed about 91.80 to 127.45. These large molar refractivity values indicate an antagonistic behaviour for all synthesized compounds. Fragment based drug-likeness is a parameter that depends on some descriptors like topological, clog *P*, molecular weights and fingerprints of molecular design limited structure. The drug-likeness is obtained from a fragment-list

which is made by the fragmentation of 3300-traded drugs as well as 15,000 commercially available chemicals to access a complete list of all available fragments. Molecules that predominantly contain fragments that are frequently found in commercial drugs have a positive drug-likeness. Although the calculated drug-likeness parameters for title compounds displayed the negative values, this is not be disappointing since many well-established drugs like fluconazole also displayed a negative drug-likeness (Table 4). On the other hand, even when clotrimazole's clog *P*, log *S* and log *D* values were out of range, this drug displayed a positive drug-likeness record (Table 4). Drug score is a parameter that indicates if a compound could be considered as a drug candidate. Drug score combines parameters such as drug-likeness, clog *P*, log *S*, molecular weight and toxicity risks. Drug score values for **10a–10n** were in the range of 0.04–0.44 which are less than fluconazole (=0.46); however, compounds **10a**, **10c**, **10d**, **10f**, **10h** and **10j** have higher drug score values than clotrimazole. In particular, compound **10d** with an admissible drug score value (=0.44) and also an appropriate antifungal activity can be considered as a potential drug candidate.

## Conclusions

In summary, we explained the design and synthesis of a novel series of 1,2,3-triazolyl β-hydroxy alkyl/carbazole hybrid molecules (**10a–10n**) as a new type of antifungal agent. In this synthesis, the treatment of potassium carbazol-9-ide **11** with 3-bromoprop-1-yne in DMSO at room temperature led to alkyne **12** as a key precursor for

'Click' synthesis of **10a–10n**. Finally, CDSCS catalyzed the cycloaddition reaction of alkyne **12** with  $\beta$ -azido alcohols **13a–13n** afforded the target molecules in racemic form. The in vitro antifungal and antibacterial activities of **10a–10n** were examined against several pathogenic fungi, Gram-positive and/or Gram-negative bacteria. The biological investigation revealed that compound **10e** was the most potent agent against all examined fungal pathogens and its activity was comparable to fluconazole and clotrimazole. Docking analysis predicts strong binding of **10e** in the active site of Mycobacterium P450DM enzyme and its binding is considerably higher than fluconazole. In addition, molecular modelling indicates that the inhibition of Mycobacterium P450DM via **10e** was achieved through an interaction which is different from fluconazole–Mycobacterium P450DM enzyme interaction. The in silico pharmacokinetic profile, drug-likeness and toxicity predictions performed for all compounds determined that compounds **10e** and **10d** can be considered as potential drug candidates for future research.

## Experimental

### General

All materials were purchased from either Fluka or Merck except that of copper-doped silica cuprous sulphate (CDSCS) which was prepared according to the literature [37]. Solvents were purified using standard procedures and stored over 3 Å molecular sieves. Reactions were monitored by TLC using SILG/UV 254 silica-gel plates. Column chromatography was performed on silica gel 60 (0.063–0.200 mm, 70–230 mesh; ASTM). Melting points were measured using Electrothermal IA 9000 melting point apparatus in open capillary tubes and are uncorrected. IR spectra were obtained using a Shimadzu FT-IR-8300 spectrophotometer.  $^1\text{H}$ - and  $^{13}\text{C}$ -NMR spectra were recorded on a Bruker Avance-DPX-250 spectrometer operating at 250/62.5 MHz, respectively. Chemical shifts are given in  $\delta$  relative to tetramethylsilane (TMS) as an internal standard, coupling constants  $J$  are given in Hz. Abbreviations used for  $^1\text{H}$  NMR signals are *s* singlet, *d* doublet, *t* triplet, *q* quartet, *m* multiplet, *b* broad, *dd* doublet of doublet. GC/MS was performed on a Shimadzu GC/MS-QP 1000-EX apparatus (*m/z*; rel. %). Elemental analyses were performed on a Perkin–Elmer 240-B microanalyzer.

### Preparation of potassium carbazol-9-ide **11**

In a round-bottomed flask (100 mL), a mixture of 9*H*-carbazole (1.67 g, 0.01 mol) and KOH (0.67 g, 0.012 mol) in EtOH (40 mL) was heated at 70 °C for 4 h (TLC control). The

solvent was then evaporated and dried to afford compound **11** as a bright brown solid which was used in the next step without further purification.

### Synthesis of 9-(prop-2-ynyl)-9*H*-carbazole **12**

In a round-bottomed flask (100 mL), 3-bromoprop-1-yne (1.55 g, 0.013 mol) was added dropwise to a solution of potassium carbazol-9-ide (2.05 g, 0.01 mol) in DMSO (15 mL). The mixture was stirred at room temperature for 3 h (TLC control). Then, the crude product was dissolved in  $\text{CHCl}_3$  (100 mL) and washed with  $\text{H}_2\text{O}$  (3  $\times$  150 mL). The organic layer was dried (10 g of  $\text{Na}_2\text{SO}_4$ ) and concentrated to afford the corresponding product. The crude product was purified by column chromatography on silica gel eluting with EtOAc-*n*-hexane (1:8) which yielded 1.93 g (94 %) of **12** as a pale-yellow solid, mp: 173–175 °C (Lit. [42]: 172–174 °C).

### General procedure for the synthesis of $\beta$ -azido alcohols **13a–13n**

The  $\beta$ -azido Alcohols **13a–13n** were prepared by our previously described method in the literature [37,38].

### General procedure for the synthesis of 1,2,3-triazolyl $\beta$ -hydroxy alkyl/carbazole hybrid **10a–10n**

In a round-bottomed flask (100 mL), a mixture of alkyne **12** (2.05 g, 0.01 mol), appropriate  $\beta$ -azido alcohol (0.012 mol) and CDSCS (0.3 g, 0.05 mol%) in THF/ $\text{H}_2\text{O}$  (1:1 v/v, 20 mL) was stirred at room temperature until TLC monitoring indicated no further progress of the reaction (0.6–1 h). The catalyst was then filtered off, washed with THF/ $\text{H}_2\text{O}$  (5  $\times$  10 mL) and the filtrate was evaporated under vacuum to remove the solvent. The remaining foam was dissolved in  $\text{CHCl}_3$  (100 mL) and subsequently washed with water (2  $\times$  100 mL). The organic layer was dried ( $\text{Na}_2\text{SO}_4$ ) and evaporated. The crude product was purified by column chromatography on silica gel eluting with proper solvents.

### 2-(4-((9*H*-Carbazol-9-yl)methyl)-1*H*-1,2,3-triazol-1-yl) cyclohexanol (**10a**)

Column chromatography on silica gel (EtOAc-*n*-hexane, 1:2) gave compound **10a** as a white solid (2.91 g, 84 %). mp: 196–197 °C;  $^1\text{H}$  NMR (250 MHz,  $\text{CDCl}_3$ ):  $\delta$  = 1.26–1.34 (m, 4H, 2 $\text{CH}_2$ ), 1.65–1.75 (m, 4H, 2 $\text{CH}_2$ ), 2.82 (s, 1H, OH), 3.81–3.92 (m, 2H, *NCHCHOH*), 5.51 (s, 2H, *NCH}\_2\text{C} = \text{C}*), 7.20–7.44 (m, 8H, Ar-H), 8.05 ppm (s, 1H, C(5)-H of triazole);  $^{13}\text{C}$  NMR (62.5 MHz,  $\text{CDCl}_3$ ):  $\delta$  = 22.3, 24.5, 27.3, 32.0, 58.7, 63.6, 68.7, 112.5, 118.2, 119.4, 120.4, 122.5, 123.5, 131.3, 142.3 ppm; IR (KBr):  $\nu$  = 3230, 3069, 2957, 1482  $\text{cm}^{-1}$ ; MS (*m/z*, %): 346 (21.7,

M<sup>+</sup>); Anal. calcd for C<sub>21</sub>H<sub>22</sub>N<sub>4</sub>O: C 72.81, H 6.40, N 16.17, found: C 72.89, H 6.53, N 16.25.

**1-(4-((9H-Carbazol-9-yl)methyl)-1H-1,2,3-triazol-1-yl)propan-2-ol (10b)**

Column chromatography on silica gel (EtOAc-*n*-hexane, 2:1) gave compound **10b** as a white solid (2.66 g, 87%). mp: 160–161 °C; <sup>1</sup>H NMR (250 MHz, CDCl<sub>3</sub>): δ = 0.95 (d, *J* = 5.9 Hz, 3H, CH<sub>3</sub>), 2.95 (s, 1H, OH), 3.77–3.90 (m, 3H, NCH<sub>2</sub>CH), 5.36 (s, 2H, NCH<sub>2</sub>C = C), 7.04–7.13 (m, 4H, Ar-H), 7.28–7.30 (m, 4H, Ar-H), 7.92 ppm (s, 1H, C(5)-H of triazole); <sup>13</sup>C NMR (62.5 MHz, CDCl<sub>3</sub>): δ = 23.1, 63.3, 64.9, 69.4, 112.5, 118.8, 119.8, 120.1, 122.4, 123.4, 130.4, 144.1 ppm; IR (KBr): ν = 3395, 3104, 2934, 1463 cm<sup>-1</sup>; MS (m/z, %): 306 (19.4, M<sup>+</sup>); Anal. calcd for C<sub>18</sub>H<sub>18</sub>N<sub>4</sub>O: C 70.57, H 5.92, N 18.29, found: C 70.68, H 6.05, N 18.20.

**1-(4-((9H-Carbazol-9-yl)methyl)-1H-1,2,3-triazol-1-yl)butan-2-ol (10c)**

Column chromatography on silica gel (EtOAc-*n*-hexane, 2:1) gave compound **10c** as a creamy solid (2.75 g, 86%). mp: 118–119 °C; <sup>1</sup>H NMR (250 MHz, CDCl<sub>3</sub>): δ = 0.86 (t, *J* = 7.5 Hz, 3H, CH<sub>3</sub>), 1.31–1.36 (m, 2H, CH<sub>2</sub>CH<sub>3</sub>), 2.93 (s, 1H, OH), 3.67–3.74 (m, 1H, CHOH), 3.88–3.94 (m, 1H, NCH<sub>A</sub>H<sub>B</sub>CH), 4.12 (dd, *J* = 2.5, 12.5 Hz, 1H, NCH<sub>A</sub>H<sub>B</sub>CH), 5.45 (s, 2H, NCH<sub>2</sub>C = C), 7.16–7.40 (m, 8H, Ar-H), 8.01 ppm (s, 1H, C(5)-H of triazole); <sup>13</sup>C NMR (62.5 MHz, CDCl<sub>3</sub>): δ = 9.3, 29.8, 61.7, 64.4, 70.7, 112.9, 119.2, 120.1, 121.6, 123.4, 124.6, 131.8, 145.2 ppm; IR (KBr): ν = 3342, 3049, 2960, 1442 cm<sup>-1</sup>; MS (m/z, %): 320 (18.1, M<sup>+</sup>); Anal. calcd for C<sub>19</sub>H<sub>20</sub>N<sub>4</sub>O: C 71.23, H 6.29, N 17.49, found: C 71.31, H 6.38, N 17.40.

**1-(4-((9H-Carbazol-9-yl)methyl)-1H-1,2,3-triazol-1-yl)-2-methylpropan-2-ol (10d)**

Column chromatography on silica gel (EtOAc-*n*-hexane, 2:1) gave compound **10d** as a white solid (2.72 g, 85%). mp: 114–115 °C; <sup>1</sup>H NMR (250 MHz, CDCl<sub>3</sub>): δ = 1.03 (s, 6H, 2CH<sub>3</sub>), 2.75 (s, 1H, OH), 3.99 (s, 2H, NCH<sub>2</sub>C), 5.48 (s, 2H, NCH<sub>2</sub>C = C), 7.17–7.21 (m, 4H, Ar-H), 7.35–7.40 (m, 4H, Ar-H), 8.01 ppm (s, 1H, C(5)-H of triazole); <sup>13</sup>C NMR (62.5 MHz, CDCl<sub>3</sub>): δ = 29.8, 64.2, 66.2, 68.8, 111.8, 118.4, 119.3, 121.6, 123.3, 124.5, 131.4, 145.5 ppm; IR (KBr): ν = 3358, 3015, 2935, 1463 cm<sup>-1</sup>; MS (m/z, %): 320 (21.7, M<sup>+</sup>); Anal. calcd for C<sub>19</sub>H<sub>20</sub>N<sub>4</sub>O: C 71.23, H 6.29, N 17.49, found: C 71.29, H 6.34, N 17.42.

**1-(4-((9H-Carbazol-9-yl)methyl)-1H-1,2,3-triazol-1-yl)-3-butoxypropan-2-ol (10e)**

Column chromatography on silica gel (EtOAc-*n*-hexane, 1:1) gave compound **10e** as a brown oil (3.40 g, 90%). <sup>1</sup>H NMR (250 MHz, CDCl<sub>3</sub>): δ = 0.93 (t, *J* = 7.5 Hz, 3H, CH<sub>3</sub>), 1.35–1.42 (m, 2H, CH<sub>2</sub>CH<sub>3</sub>), 1.55–1.58 (m, 2H, OCH<sub>2</sub>CH<sub>2</sub>), 2.53 (s, 1H, OH), 3.27 (t, *J* = 5.0 Hz, 2H, OCH<sub>2</sub>CH<sub>2</sub>), 3.37–3.39 (m, 2H, OCH<sub>2</sub>CH), 4.20–4.22 (m, 1H, CHOH), 4.34–4.39 (m, 2H, NCH<sub>2</sub>CH), 5.08 (s, 2H, NCH<sub>2</sub>C = C), 7.20–7.23 (m, 4H, Ar-H), 7.43–7.45 (m, 4H, Ar-H), 8.04 ppm (s, 1H, C(5)-H of triazole); <sup>13</sup>C NMR (62.5 MHz, CDCl<sub>3</sub>): δ = 14.8, 21.4, 33.3, 58.1, 64.4, 66.5, 73.1, 75.2, 111.9, 118.8, 120.3, 121.5, 122.7, 123.5, 131.3, 143.5 ppm; IR (film): ν = 3450, 3025, 2963, 1472, 1241 cm<sup>-1</sup>; MS (m/z, %): 378 (26.1, M<sup>+</sup>); Anal. calcd for C<sub>22</sub>H<sub>26</sub>N<sub>4</sub>O<sub>2</sub>: C 69.82, H 6.92, N 14.80, found: C 69.71, H 6.98, N 14.86.

**1-(4-((9H-Carbazol-9-yl)methyl)-1H-1,2,3-triazol-1-yl)-3-isopropoxypropan-2-ol (10f)**

Column chromatography on silica gel (EtOAc-*n*-hexane, 2:1) gave compound **10f** as a creamy solid (3.32 g, 91%). mp: 112–113 °C; <sup>1</sup>H NMR (250 MHz, CDCl<sub>3</sub>): δ = 0.99 (d, *J* = 7.7 Hz, 6H, 2CH<sub>3</sub>), 3.11–3.17 (m, 2H, OCH<sub>2</sub>), 3.23–3.27 (m, 1H, CHOH), 3.37 (sept, *J* = 6.0 Hz, 1H, CH(CH<sub>3</sub>)<sub>2</sub>), 3.96 (s, 1H, OH), 4.13 (dd, *J* = 6.7, 12.5 Hz, 1H, NCH<sub>A</sub>H<sub>B</sub>CH), 4.26 (dd, *J* = 3.7, 14.0 Hz, 1H, NCH<sub>A</sub>H<sub>B</sub>CH), 5.52 (s, 2H, NCH<sub>2</sub>C = C), 7.17–7.23 (m, 4H, Ar-H), 7.37–7.41 (m, 4H, Ar-H), 8.03 ppm (s, 1H, C(5)-H of triazole); <sup>13</sup>C NMR (62.5 MHz, CDCl<sub>3</sub>): δ = 25.6, 58.1, 64.0, 67.6, 72.6, 73.7, 112.4, 117.5, 119.1, 120.5, 122.7, 124.1, 131.1, 144.8 ppm; IR (KBr): ν = 3556, 3018, 2938, 1452, 1237 cm<sup>-1</sup>; MS (m/z, %): 364 (22.5, M<sup>+</sup>); Anal. calcd for C<sub>21</sub>H<sub>24</sub>N<sub>4</sub>O<sub>2</sub>: C 69.21, H 6.64, N 15.37, found: C 69.35, H 6.72, N 15.30.

**3-(4-((9H-Carbazol-9-yl)methyl)-1H-1,2,3-triazol-1-yl)-2-hydroxypropyl methacrylate (10g)**

Column chromatography on silica gel (EtOAc-*n*-hexane, 2:1) gave compound **10g** as a creamy solid (3.43 g, 88%). mp: 119–120 °C; <sup>1</sup>H NMR (250 MHz, CDCl<sub>3</sub>): δ = 2.49 (s, 3H, CH<sub>3</sub>), 3.27–3.40 (m, 3H, NCH<sub>2</sub>CH), 3.78 (s, 1H, OH), 4.18 (dd, *J* = 8.0, 13.7 Hz, 1H, OCH<sub>A</sub>H<sub>B</sub>), 4.44 (dd, *J* = 3.2, 13.7 Hz, 1H, OCH<sub>A</sub>H<sub>B</sub>), 4.86 (d, *J* = 5.3 Hz, 1H, = CH<sub>A</sub>H<sub>B</sub>), 5.11 (d, *J* = 5.3 Hz, 1H, = CH<sub>A</sub>H<sub>B</sub>), 5.68 (s, 2H, NCH<sub>2</sub>C = C), 7.20–7.24 (m, 2H, Ar-H), 7.46–7.50 (m, 2H, Ar-H), 7.81 (d, *J* = 8.2 Hz, 2H, Ar-H), 7.99 (s, 1H, C(5)-H of triazole), 8.15 ppm (d, *J* = 7.8 Hz, 2H, Ar-H); <sup>13</sup>C NMR (62.5 MHz, CDCl<sub>3</sub>): δ = 18.6, 58.5, 63.7, 65.9, 70.5, 111.3, 118.3, 119.3, 120.8, 122.0, 123.2, 126.9, 131.1, 137.8, 143.6, 169.6 ppm; IR (KBr): ν = 3327, 3050, 2972, 1724, 1473,

1267  $\text{cm}^{-1}$ ; MS ( $m/z$ , %): 390 (28.9,  $M^+$ ); Anal. calcd for  $\text{C}_{22}\text{H}_{22}\text{N}_4\text{O}_3$ : C 67.68, H 5.68, N 14.35, found: C 67.57, H 5.73, N 14.27.

**1-(4-((9H-Carbazol-9-yl)methyl)-1H-1,2,3-triazol-1-yl)-3-phenoxypropan-2-ol (10h)**

Column chromatography on silica gel (EtOAc-*n*-hexane, 2:1) gave compound **10h** as a creamy solid (3.66 g, 92 %). mp: 158–159 °C;  $^1\text{H}$  NMR (250 MHz,  $\text{CDCl}_3$ ):  $\delta$  = 3.95 (d,  $J$  = 4.8 Hz, 2H,  $\text{NCH}_2\text{CH}$ ), 4.22–4.23 (m, 1H,  $\text{CHOH}$ ), 4.41 (s, 1H, OH), 4.46 (dd,  $J$  = 7.0, 13.4 Hz, 1H,  $\text{OCH}_A\text{H}_B$ ), 4.66 (dd,  $J$  = 2.5, 13.2 Hz, 1H,  $\text{OCH}_A\text{H}_B$ ), 5.09 (s, 2H,  $\text{NCH}_2\text{C} = \text{C}$ ), 6.83–6.85 (m, 5H, Ar-H), 7.13–7.25 (m, 8H, Ar-H), 7.92 ppm (s, 1H, C(5)-H of triazole);  $^{13}\text{C}$  NMR (62.5 MHz,  $\text{CDCl}_3$ ):  $\delta$  = 57.1, 64.9, 66.5, 72.4, 111.9, 115.0, 117.5, 118.8, 119.7, 120.4, 121.9, 123.2, 128.8, 130.4, 144.2, 158.9 ppm; IR (KBr):  $\nu$  = 3264, 3050, 2925, 1463, 1239  $\text{cm}^{-1}$ ; MS ( $m/z$ , %): 398 (25.6,  $M^+$ ); Anal. calcd for  $\text{C}_{24}\text{H}_{22}\text{N}_4\text{O}_2$ : C 72.34, H 5.57, N 14.06, found: C 72.23, H 5.50, N 14.17.

**1-(4-((9H-Carbazol-9-yl)methyl)-1H-1,2,3-triazol-1-yl)-3-(*p*-tolylloxy)propan-2-ol (10i)**

Column chromatography on silica gel (EtOAc-*n*-hexane, 2:1) gave compound **10i** as a brown oil (3.75 g, 91 %).  $^1\text{H}$  NMR (250 MHz,  $\text{CDCl}_3$ ):  $\delta$  = 2.15 (s, 3H,  $\text{CH}_3$ ), 3.91–3.94 (m, 2H,  $\text{NCH}_2\text{CH}$ ), 4.08–4.11 (m, 1H,  $\text{CHOH}$ ), 4.39 (s, 1H, OH), 4.45 (dd,  $J$  = 6.6, 13.7 Hz, 1H,  $\text{OCH}_A\text{H}_B$ ), 4.63 (dd,  $J$  = 6.5, 13.6 Hz, 1H,  $\text{OCH}_A\text{H}_B$ ), 5.13 (s, 2H,  $\text{NCH}_2\text{C} = \text{C}$ ), 6.79–6.88 (m, 6H, Ar-H), 7.13–7.22 (m, 6H, Ar-H), 7.77 ppm (s, 1H, C(5)-H of triazole);  $^{13}\text{C}$  NMR (62.5 MHz,  $\text{CDCl}_3$ ):  $\delta$  = 24.0, 58.2, 64.3, 65.9, 73.3, 112.5, 115.7, 118.6, 119.8, 120.5, 122.7, 124.0, 129.7, 131.0, 132.3, 144.4, 159.8 ppm; IR (film):  $\nu$  = 3379, 3058, 2923, 1468, 1276  $\text{cm}^{-1}$ ; MS ( $m/z$ , %): 412 (27.3,  $M^+$ ); Anal. calcd for  $\text{C}_{25}\text{H}_{24}\text{N}_4\text{O}_2$ : C 72.80, H 5.86, N 13.58, found: C 72.73, H 5.94, N 13.50.

**1-(4-((9H-Carbazol-9-yl)methyl)-1H-1,2,3-triazol-1-yl)-3-(4-methoxyphenoxy)propan-2-ol (10j)**

Column chromatography on silica gel (EtOAc-*n*-hexane, 3:1) gave compound **10j** as a brown solid (3.94 g, 92 %). mp: 125–126 °C;  $^1\text{H}$  NMR (250 MHz,  $\text{CDCl}_3$ ):  $\delta$  = 2.05 (s, 3H,  $\text{OCH}_3$ ), 3.94 (dd,  $J$  = 5.0, 10.2 Hz, 2H,  $\text{NCH}_2\text{CH}$ ), 4.04 (s, 1H, OH), 4.12–4.18 (m, 3H,  $\text{OCH}_2$ ,  $\text{CHOH}$ ), 5.70 (s, 2H,  $\text{NCH}_2\text{C} = \text{C}$ ), 6.67–6.77 (m, 4H, Ar-H), 7.20–7.23 (m, 4H, Ar-H), 7.41–7.46 (m, 4H, Ar-H), 8.06 ppm (s, 1H, C(5)-H of triazole);  $^{13}\text{C}$  NMR (62.5 MHz,  $\text{CDCl}_3$ ):  $\delta$  = 56.0, 58.1, 62.3, 65.9, 71.0, 112.3, 115.6, 116.8, 118.9, 120.1, 121.6, 123.1, 124.3, 131.8, 144.0, 150.3, 159.9 ppm; IR (KBr):  $\nu$  = 3235, 3045, 2948, 1462, 1246  $\text{cm}^{-1}$ ; MS ( $m/z$ , %): 428

(29.4,  $M^+$ ); Anal. calcd for  $\text{C}_{25}\text{H}_{24}\text{N}_4\text{O}_3$ : C 70.08, H 5.65, N 13.08, found: C 69.98, H 5.73, N 13.16.

**1-(4-((9H-Carbazol-9-yl)methyl)-1H-1,2,3-triazol-1-yl)-3-(4-chloro-3-methylphenoxy)propan-2-ol (10k)**

Column chromatography on silica gel (EtOAc-*n*-hexane, 2:1) gave compound **10k** as a creamy solid (3.89 g, 87 %). mp: 167–168 °C;  $^1\text{H}$  NMR (250 MHz,  $\text{CDCl}_3$ ):  $\delta$  = 2.25 (s, 3H,  $\text{CH}_3$ ), 3.96–3.98 (m, 2H,  $\text{NCH}_2\text{CH}$ ), 4.22 (s, 1H, OH), 4.49–4.71 (m, 3H,  $\text{OCH}_2$ ,  $\text{CHOH}$ ), 5.09 (s, 2H,  $\text{NCH}_2\text{C} = \text{C}$ ), 6.81–6.85 (m, 3H, Ar-H), 7.13–7.30 (m, 8H, Ar-H), 7.77 ppm (s, 1H, C(5)-H of triazole);  $^{13}\text{C}$  NMR (62.5 MHz,  $\text{CDCl}_3$ ):  $\delta$  = 20.4, 58.7, 63.9, 66.8, 71.4, 111.5, 113.5, 117.6, 119.9, 120.7, 121.6, 122.8, 123.3, 125.9, 130.2, 131.7, 137.5, 144.4, 157.4 ppm; IR (KBr):  $\nu$  = 3391, 3029, 2953, 1456, 1258, 762  $\text{cm}^{-1}$ ; MS ( $m/z$ , %): 446 (30.8,  $M^+$ ); Anal. calcd for  $\text{C}_{25}\text{H}_{23}\text{ClN}_4\text{O}_2$ : C 67.18, H 5.19, Cl 7.93, N 12.54, found: C 67.25, H 5.29, Cl 8.02, N 12.65.

**1-(4-((9H-Carbazol-9-yl)methyl)-1H-1,2,3-triazol-1-yl)-3-(4-chlorophenoxy)propan-2-ol (10l)**

Column chromatography on silica gel (EtOAc-*n*-hexane, 2:1) gave compound **10l** as a creamy solid (3.94 g, 91 %). mp: 110–111 °C;  $^1\text{H}$  NMR (250 MHz,  $\text{CDCl}_3$ ):  $\delta$  = 3.55 (d,  $J$  = 5.0 Hz, 1H,  $\text{NCH}_A\text{H}_B\text{CH}$ ), 3.63 (s, 1H, OH), 3.78 (d,  $J$  = 5.0 Hz, 1H,  $\text{NCH}_A\text{H}_B\text{CH}$ ), 4.05 (dd,  $J$  = 5.0, 17.5 Hz, 2H,  $\text{OCH}_2$ ), 4.19–4.21 (m, 1H,  $\text{CHOH}$ ), 5.33 (s, 2H,  $\text{NCH}_2\text{C} = \text{C}$ ), 6.48–6.62 (m, 4H, Ar-H), 7.03–7.11 (m, 8H, Ar-H), 7.90 ppm (s, 1H, C(5)-H of triazole);  $^{13}\text{C}$  NMR (62.5 MHz,  $\text{CDCl}_3$ ):  $\delta$  = 59.6, 64.4, 65.9, 72.8, 113.1, 116.7, 118.5, 119.7, 120.6, 122.1, 124.2, 126.0, 130.2, 131.7, 144.8, 157.3 ppm; IR (KBr):  $\nu$  = 3228, 3100, 2937, 1595, 1228, 755  $\text{cm}^{-1}$ ; MS ( $m/z$ , %): 432 (28.4,  $M^+$ ); Anal. calcd for  $\text{C}_{24}\text{H}_{21}\text{ClN}_4\text{O}_2$ : C 66.59, H 4.89, Cl 8.19, N 12.94, found: C 66.48, H 4.80, Cl 8.26, N 13.04.

**1-(4-((9H-Carbazol-9-yl)methyl)-1H-1,2,3-triazol-1-yl)-3-(2-chlorophenoxy)propan-2-ol (10m)**

Column chromatography on silica gel (EtOAc-*n*-hexane, 2:1) gave compound **10m** as a brown oil (3.85 g, 89 %).  $^1\text{H}$  NMR (250 MHz,  $\text{CDCl}_3$ ):  $\delta$  = 3.86–3.90 (m, 3H,  $\text{NCH}_2\text{CH}$ ), 4.21 (s, 1H, OH), 4.44 (dd,  $J$  = 7.6, 13.8 Hz, 1H,  $\text{OCH}_A\text{H}_B$ ), 4.59 (dd,  $J$  = 3.4, 13.8 Hz, 1H,  $\text{OCH}_A\text{H}_B$ ), 5.13 (s, 2H,  $\text{NCH}_2\text{C} = \text{C}$ ), 6.85 (d,  $J$  = 8.3 Hz, 2H, Ar-H), 7.07–7.29 (m, 10H, Ar-H), 8.18 ppm (s, 1H, C(5)-H of triazole);  $^{13}\text{C}$  NMR (62.5 MHz,  $\text{CDCl}_3$ ):  $\delta$  = 58.5, 64.8, 67.4, 70.7, 112.8, 116.6, 118.6, 119.4, 120.5, 121.6, 122.2, 123.0, 123.8, 128.0, 130.0, 131.7, 143.6, 151.5 ppm; IR (film):  $\nu$  = 3423, 3026, 2981, 1486, 1263, 759  $\text{cm}^{-1}$ ; MS ( $m/z$ , %): 432 (30.1,  $M^+$ ); Anal. calcd for  $\text{C}_{24}\text{H}_{21}\text{ClN}_4\text{O}_2$ : C 66.59, H 4.89, Cl 8.19, N 12.94, found: C 66.64, H 4.96, Cl 8.31, N 13.01.

### 1-(4-((9H-Carbazol-9-yl)methyl)-1H-1,2,3-triazol-1-yl)-3-(2,4-dichlorophenoxy)propan-2-ol (10n)

Column chromatography on silica gel (EtOAc-*n*-hexane, 2:1) gave compound **10n** as a white solid (4.20 g, 90 %). mp: 115 – 116 °C; <sup>1</sup>H NMR (250 MHz, CDCl<sub>3</sub>) : δ = 3.63 (d, *J* = 4.8 Hz, 2H, NCH<sub>2</sub>CH), 3.91 (s, 1H, OH), 4.15–4.28 (m, 3H, OCH<sub>2</sub>, CHOH), 5.38 (s, 2H, NCH<sub>2</sub>C = C), 6.48 (d, *J* = 8.8 Hz, 1H, Ar-H), 6.96–6.98 (m, 1H, Ar-H), 7.11–7.19 (m, 3H, Ar-H), 7.32–7.43 (m, 5H, Ar-H), 7.95 (s, 1H, Ar-H), 7.99 ppm (s, 1H, C(5)-H of triazole); <sup>13</sup>C NMR (62.5 MHz, CDCl<sub>3</sub>): δ = 58.2, 64.0, 67.4, 71.0, 113.5, 118.6, 119.5, 120.1, 121.1, 122.0, 123.8, 125.0, 127.5, 128.1, 130.2, 132.1, 144.0, 150.1 ppm; IR (KBr): ν = 3396, 3050, 2935, 1479, 1238, 761 cm<sup>-1</sup>; MS (m/z, %): 467 (34.5, M<sup>+</sup>); Anal. calcd for C<sub>24</sub>H<sub>20</sub>Cl<sub>2</sub>N<sub>4</sub>O<sub>2</sub>: C 61.68, H 4.31, Cl 15.17, N 11.99, found: C 61.60, H 4.38, Cl 15.24, N 11.

**Acknowledgments** The authors wish to thank Shiraz University of Technology research council for partial support of this work.

#### Compliance with ethical standards

**Conflict of interest** The authors declare that they have no conflict of interest.

#### References

- Emori TG, Gaynes RP (1993) An overview of nosocomial infections, including the role of the microbiology laboratory. *Clin Microbiol Rev* 6:428–442. doi:10.1128/CMR.6.4.428
- Pappas PG (2011) The role of azoles in the treatment of invasive mycoses: review of the infectious diseases society of America guidelines. *Curr Opin Infect Dis* 24:S1–S13. doi:10.1097/OI.qco.0000399602.83515.ac
- Rüping MJ, Vehreschild JJ, Cornely OA (2008) Patients at high risk of invasive fungal infections. *Drugs* 68:1941–1962. doi:10.2165/00003495-200868140-00002
- Jain A, Jain S, Rawat S (2010) Emerging fungal infections among children: a review on its clinical manifestations, diagnosis, and prevention. *J Pharm Bioallied Sci* 2:314–320. doi:10.4103/0975-7406.72131
- Sorbera LA, Aravamudan J, Rosa E (2011) Therapeutic targets for candidiasis. *Drugs Future* 36:627–630. doi:10.1358/dof.2011.36.8.1686467
- Kleeman A, Engel J, Kutscher B, Reichert D (1999) *Pharmaceutical substances*, 3rd edn. Thieme, Stuttgart
- Behbehani H, Ibrahim HM, Makhseed S, Mahmoud H (2011) Applications of 2-arylhydrazono nitriles in synthesis: preparation of new indole containing 1,2,3-triazole, pyrazole and pyrazolo[1,5-a]pyrimidine derivatives and evaluation of their antimicrobial activities. *Eur J Med Chem* 46:1813–1820. doi:10.1016/j.ejmech.2011.02.040
- Johnson DS, Li JJ (2007) *The art of drug synthesis*. Wiley, Hoboken
- Kunzler A, Neuenfeldt PD, das Neves AM, Pereira CMP, Marques GH, Nascente PS, Fernandes MHV, Hübner SO (2013) Synthesis, antifungal and cytotoxic activities of 2-aryl-3-((piperidin-1-yl)ethyl)thiazolidinones. *Eur J Med Chem* 64:74–80. doi:10.1016/j.ejmech.2013.03.030
- Xu Y, Sheng C, Wang W, Che X, Cao Y, Dong G, Wang S, Ji H, Miao Z, Yao J, Zhang W (2010) Structure-based rational design, synthesis and antifungal activity of oxime-containing azole derivatives. *Bioorg Med Chem Lett* 20:2942–2945. doi:10.1016/j.bmcl.2010.03.014
- Kathiravan MK, Salake AB, Chothe AS, Dudhe PB, Watode RP, Mukta MS, Gadhwe S (2012) The biology and chemistry of antifungal agents: a review. *Bioorg Med Chem* 20:5678–5698. doi:10.1016/j.bmc.2012.04.045
- Odds F, Brown AJP, Gow NAR (2003) Antifungal agents: mechanisms of action. *Trends Microbiol* 11:272–279. doi:10.1016/S0966-842X(03)00117-3
- Strushkevich N, Usanov SA (2010) Structural basis of human CYP51 inhibition by antifungal azoles. *J Mol Biol* 397:1067–1078. doi:10.1016/j.jmb.2010.01.075
- Rostovtsev VV, Green LG, Fokin VV, Sharples KB (2002) A step-wise Huisgen cycloaddition process: copper(I)-catalyzed regioselective “ligation” of azides and terminal alkynes. *Angew Chem Int Ed* 41:2596–2599
- Tornøe CW, Christensen C, Meldal M (2002) Peptidotriazoles on solid phase: [1,2,3]-triazoles by regiospecific copper(I)-catalyzed 1,3-dipolar cycloadditions of terminal alkynes to azides. *J Org Chem* 67:3057–3064. doi:10.1021/jo011148
- Haider S, Alam MS, Hamid H (2014) 1, 2, 3-Triazoles: scaffold with medicinal significance. *Inflamm Cell Signal* 1:e95. doi:10.14800/ics.95
- Moses JE, Moorhouse AD (2007) The growing applications of click chemistry. *Chem Soc Rev* 36:1249–1262. doi:10.1039/B613014N
- Zhou CH, Wang Y (2012) Recent researches in triazole compounds as medicinal drugs. *Curr Med Chem* 19:239–280. doi:10.2174/092986712803414213
- Meunier B (2008) Hybrid molecules with a dual mode of action: dream or reality? *Acc Chem Res* 41:69–77. doi:10.1021/ar7000843
- Muregi FW, Ishih A (2010) Next-generation antimalarial drugs: hybrid molecules as a new strategy in drug design. *Drug Dev Res* 71:20–32. doi:10.1002/ddr.20345
- Letribot B, Akué-Gédu R, Santio NM, El-Ghozzi M, Avignant D, Cisnetti F, Koskinen PJ, Gautier A, Anizon F, Moreau P (2012) Use of copper(I) catalyzed azide alkyne cycloaddition (CuAAC) for the preparation of conjugated pyrrolo[2,3-a]carbazole Pim kinase inhibitors. *Eur J Med Chem* 2012:304–310. doi:10.1016/j.ejmech.2012.02.009
- Akrami H, Mirjalili BF, Khoobi M, Moradi A, Nadri H, Emami S, Foroumadi A, Vosooghi M, Shafiee A (2015) 9H-Carbazole derivatives containing the N-benzyl-1,2,3-triazole moiety as new acetylcholinesterase inhibitors. *Arch Pharm Chem Life Sci* 348:366–374. doi:10.1002/ardp.201400365
- Silva M, Gonçalves JCO, Oliveira-Campos AMF, Rodrigues LM, Esteves AP (2013) Synthesis of novel glycoconjugates derived from alkynyl heterocycles through a click approach. *Synth Commun* 43:1432–1438. doi:10.1080/00397911.2011.637655
- Ameen MA, El-Shaieb KM, Mohamed AH, Abdel-Latif FF (2015) Exploiting the 1,2,3-triazole moiety to generate carbazole molecular architectures through click approach. *J Heterocycl Chem* 52:1718–1722. doi:10.1002/jhet.1966
- Patpi SR, Pulipati L, Yogeewari P, Sriram D, Jain N, Sridhar B, Murthy R, Devi TA, Kalivendi SV, Kantevari S (2012) Design, synthesis, and structure-activity correlations of novel dibenzo[b, d]furan, dibenzo[b, d]thiophene, and N-methylcarbazole clubbed 1,2,3-triazoles as potent inhibitors of Mycobacterium tuberculosis. *J Med Chem* 55:3911–3922. doi:10.1021/jm300125e
- Surineni G, Yogeewari P, Sriram D, Kantevari S (2015) Rational design, synthesis and evaluation of novel-substituted 1,2,3-triazolymethyl carbazoles as potent inhibitors of Mycobacterium tuberculosis. *Med Chem Res* 24:1298–1309. doi:10.1007/s00044-014-1210-y

27. Hung WY, Tu GM, Chena SW, Chi Y (2012) Phenylcarbazole-dipyridyl triazole hybrid as bipolar host material for phosphorescent OLEDs. *J Mater Chem* 22:5410–5418. doi:10.1039/c2jm15963e
28. Bahy A, Chemli M, Ben Hassine B (2013) Synthesis and characterization of new carbazole-based materials for optoelectronic applications. *Tetrahedron Lett* 54:4026–4029. doi:10.1016/j.tetlet.2013.05.091
29. Zhuang J, Li W, Su W, Zhou M, Cui Z (2014) Novel ternary bipolar host material with carbazole, triazole and phosphine oxide moieties for high efficiency sky-blue OLEDs. *New J Chem* 38:650–656. doi:10.1039/c3nj01054f
30. Shi L, Jia N, Kong L, Qi S, Wu D (2014) Tuning resistive switching memory behavior from non-volatile to volatile by phenoxy linkages in soluble polyimides containing carbazole-tethered triazole groups. *Macromol Chem Phys* 215:2374–2388. doi:10.1002/macp.201400441
31. Zhang FF, Gan LL, Zhou CH (2010) Synthesis, antibacterial and antifungal activities of some carbazole derivatives. *Bioorg Med Chem Lett* 20:1881–1884. doi:10.1016/j.bmcl.2010.01.159
32. Zhu SP, Wang WY, Fang K, Li ZG, Dong GQ, Miao ZY, Yao JZ, Zhang WN, Sheng CQ (2004) Design, synthesis and antifungal activity of carbazole derivatives. *Chin Chem Lett* 25:229–233. doi:10.1016/j.ccl.2013.10.022
33. Soltani Rad MN, Khalafi-Nezhad A, Behrouz S (2009) Design and synthesis of some novel oxiconazole-like carboacyclic nucleoside analogues, as potential chemotherapeutic agents. *Helv Chim Acta* 92:1760–1774. doi:10.1002/hlca.200900051
34. Soltani Rad MN, Khalafi-Nezhad A, Behrouz S (2010) Synthesis of some novel hydrazono acyclic nucleoside analogues. *Beilstein J Org Chem* 6(49):1–8. doi:10.3762/bjoc.6.49
35. Soltani Rad MN, Asrari Z, Behrouz S, Hakimelahi GH, Khalafi-Nezhad A (2011) ‘Click synthesis’ of 1H–1,2,3-triazolyl-based oxiconazole (=1Z)-1-(2,4-dichlorophenyl)-2-(1H-imidazol-1-yl)ethanone O-[(2,4-dichlorophenyl)methyl]oxime analogs. *Helv Chim Acta* 94:2194–2206. doi:10.1002/hlca.201100189
36. Soltani Rad MN, Behrouz S, Nekoei AR, Faghih Z, Khalafi-Nezhad A (2011) Three-component synthesis of some novel N-heterocycle methyl-O-oxime ethers. *Synthesis* 24:4068–4076. doi:10.1055/s-0031-1289599
37. Soltani Rad MN, Behrouz S, Doroodmand MM, Movahediyani A (2012) Copper-doped silica cuprous sulfate (CDSCS) as a highly efficient and new heterogeneous nano catalyst for [3+2] Huisgen cycloaddition. *Tetrahedron* 68:7812–7821. doi:10.1016/j.tet.2012.07.032
38. Soltani Rad MN, Behrouz S, Karimitabar F, Khalafi-Nezhad A (2012) ‘Click synthesis’ of some novel O-substituted oximes containing 1,2,3-triazole-1,4-diyl residues as new analogs of  $\beta$ -adrenoceptor antagonists. *Helv Chim Acta* 95:491–501. doi:10.1002/hlca.201100324
39. Soltani Rad MN, Behrouz S, Movahedian A, Doroodmand MM, Ghasemi Y, Rasoul-Amini S, Rezaie R (2013) Doped nano-sized copper(I) oxide (Cu<sub>2</sub>O) on melamineformaldehyde resin: a highly efficient heterogeneous nano catalyst for ‘click’ synthesis of some novel 1H–1,2,3-triazole derivatives having antibacterial activity. *Helv Chim Acta* 96:688–701. doi:10.1002/hlca.201200224
40. Behrouz S, Soltani Rad MN, Rostami S, Behrouz M, Zarehnezhad E, Zarehnezhad A (2014) Design, synthesis, and biological activities of novel azole-bonded  $\beta$ -hydroxypropyl oxime O-ethers. *Mol Divers* 18:797–808. doi:10.1007/s11030-014-9539-1
41. Bissantz C, Kuhn B, Stahl M (2010) A medicinal chemist’s guide to molecular interactions. *J Med Chem* 53:5061–5084. doi:10.1021/jm100112j
42. Al-Kaissy WWN, Tuama SHF, Al-Majidi SMH (2013) Synthesis, characterization and evaluation of antimicrobial activity of some new acetylenic amine and 2-oxoazetidine of carbazole. *Am J Sci Ind Res* 4:389–398. doi:10.5251/ajsir.2013.4.4.389.398
43. Li C, Liu X, Yuan M, Li J, Guo Y, Xu J, Zhu M, Lv J, Liu H, Li Y (2007) Unusual fluorescence enhancement of a novel carbazolyl diacetylene bound to gold nanoparticles. *Langmuir* 23:6754–6760. doi:10.1021/la070110k
44. Das B, Reddy VS, Tehseen F, Krishnaiah M (2007) Catalyst-free highly regio- and stereoselective ring opening of epoxides and aziridines with sodium azide using poly (ethylene glycol) as an efficient reaction medium. *Synthesis* 5:666–668. doi:10.1055/s-2007-965921
45. National Committee for Clinical Laboratory Standards (1997) Reference Method for Broth Dilution Antifungal Susceptibility Testing of Yeasts; Approved Standard, NCCLS Document M27-A. National Committee for clinical laboratory Standards, Wayne, USA
46. Thomsen R, Christensen MH (2006) MolDock: a new technique for high-accuracy molecular docking. *J Med Chem* 49:3315–3321. doi:10.1021/jm051197e
47. Marcou G, Rognan D (2007) Optimizing fragment and scaffold docking by use of molecular interaction fingerprints. *J Chem Inf Model* 47:195–207. doi:10.1021/ci600342e
48. Podust LM, Poulos TL, Waterman MR (2001) Crystal structure of cytochrome P450 14 $\alpha$ -sterol demethylase (CYP51) from *Mycobacterium tuberculosis* in complex with azole inhibitors. *Proc Natl Acad Sci USA* 98:3068–3073. doi:10.1073/pnas.061562898
49. Conner KP, Vennam P, Woods CM, Krzyaniak MD, Bowman MK, Atkins WM (2012) 1,2,3-Triazole-heme interactions in cytochrome P450: functionally competent triazole-water-heme complexes. *Biochemistry* 51:6441–6457. doi:10.1021/bi300744z
50. Patrick GL (2011) An introduction to medicinal chemistry, 4th edn. Oxford University Press, Oxford
51. Bienstock RJ (2011) Library design, search methods, and applications of fragment-based drug design, vol 1076. American Chemical Society, Washington
52. Lipinski CA, Lombardo F, Dominy BW, Feeney PJ (2001) Experimental and computational approaches to estimate solubility and permeability in drug discovery and development settings. *Adv Drug Deliv Rev* 46:3–26. doi:10.1016/S0169-409X(00)00129-0
53. Lipinski CA (2004) Lead- and drug-like compounds: the rule-of-five revolution. *Drug Discov Today* 1:337–341. doi:10.1016/j.ddtec.2004.11.007
54. OSIRIS Property Explorer, Actelion Pharmaceuticals Ltd, Gewerbestrasse 16, 4123 Allschwil, Switzerland
55. Organic Chemistry Portal. Hauptstrasse 70, 4446 Buckten – Switzerland. <http://www.organic-chemistry.org/prog/peo/>. Accessed 22 July 2015
56. ACD/Labs PhysChem Batch Software. Advanced Chemistry Development, Inc., 8 King Street East, Suite 107, Toronto, Ontario, Canada M5C 1B5. <http://www.acdlabs.com/physchembatch/>. Accessed 22 July 2015
57. Marvin Chemaxon. ChemAxon Kft., Záhony u. 7, Building HX 1031 Budapest, Hungary. <http://www.chemaxon.com>. Accessed 22 July 2015
58. Molinspiration Property. Molinspiration, Nova ulica, SK-900 26 Slovensky Grob, Slovak Republic. <http://www.molinspiration.com/cgi-bin/properties>. Accessed 22 July 2015
59. Bhal SK, Kassam K, Peirson IG, Pearl GM (2007) The rule of five revisited: applying log d in place of log p in drug-likeness filters. *Mol Pharm* 4:556–560. doi:10.1021/mp0700209